Assessment and validation of aerodynamic performance results for a Natural Laminar Flow transonic wing tested in cryogenic conditions via simulation of turbulent wedges in CFD.

Royal Aeronautical Society 2016 Applied Aerodynamics Conference
Tuesday 19th – Thursday 21st July 2016
@Bristol Science Centre, Bristol, UK

Angela Styles, Aerodynamics Engineer
Airbus Operations Ltd,
Pegasus House,
Aerospace Avenue,
Filton, Bristol,
BS34 0PA

Steffen Risius,
German Aerospace Center (DLR)
Institute of Aerodynamics and Flow Technology
Bunsenstr. 10
37073 Goettingen
Germany

Abstract:
A test campaign was undertaken in the European Transonic Wind tunnel (ETW) using a large half model of an aircraft with a clean Natural Laminar Flow wing. The model was designed to:

1) Investigate surface tolerance requirements for Natural Laminar Flow aircraft
2) To validate the high speed aerodynamic design process for Natural Laminar Flow wings within Airbus and to investigate means of validating the expected performance benefit of laminar flow over and above that of a tripped turbulent wing

As part of the validation of performance predictions for a Natural Laminar Flow wing in free and tripped conditions, the drag impact of turbulent wedges on the laminar increment has to be quantified. This is because even in a facility with extremely good flow quality and sound operating procedures for Natural Laminar Flow testing, turbulent wedges due to flow contamination or leakage at model joints can occur that reduce the laminar extent on the wing during the course of a test run.
An investigation to compare Computational Fluid Dynamics (CFD) simulations of the Natural Laminar Flow wing in free and fixed transition cases with results obtained from the ETW test was undertaken.
The investigation showed that CFD simulations could replicate the drag increment due to upper surface laminarity measured in ETW, provided that the turbulent wedges observed in the tunnel for a given condition were modelled.

The model and the test:
The model was designed to be an approximate representation of a typical transonic short range aircraft at 1:11.5 scale, designed to cruise at a Mach number of 0.75 and Reynolds number of 25 million. The wing was designed to exhibit extensive regions of laminar flow over the bulk of its upper surface across a broad range of operating conditions. It was assumed that lower surface laminar flow would not be utilised due to the likely presence of devices for high lift performance on a real aircraft. In any case, the lower surface was tripped at the leading edge joint location on the lower surface to ensure minimal Natural Laminar Flow.
The model was equipped with a large area of Temperature Sensitive Paint (TSP) to assess transition position and also four line of flight pressure tapping stations located at 24.3%, 51.4%, 76.4% and 86.7% to verify the wing pressure distributions and provide input to post-test analysis of transition behaviour.

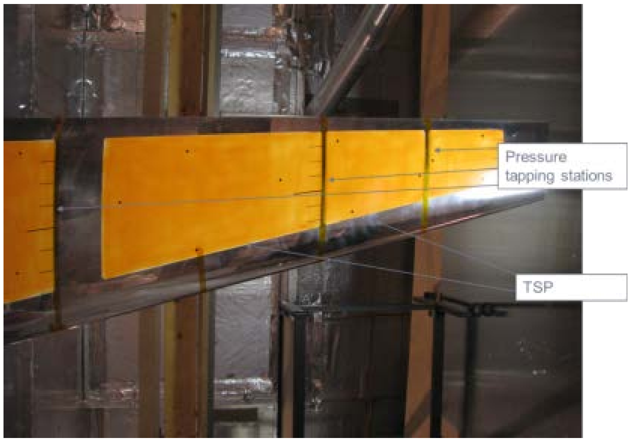

Figure 1: Image of the upper surface of the wing at ETW during model preparation, showing the upper surface TSP zones and pressure tapping stations.

The model was then assessed in cryogenic conditions at ETW through a series of continuous traverse polars to measure lift, drag and pitching moment for a range of angles of incidence. Many runs were also performed at stable lift co-efficient, Reynolds number and Mach number conditions with a brief perturbation of conditions to allow TSP images to be obtained giving the transition position for those conditions.
In addition, several runs were performed with transition fixed at the forward boundary of the TSP pocket to provide a reference turbulent dataset against which to compare the laminar performance benefit.
Achieving a wedge free image in the tunnel at high Reynolds number is very challenging. During the course of the early test entries of the model, ETW personnel worked extensively with Airbus to develop sound model preparation and testing techniques.
In subsequent test entries, images were obtained that showed a stable, small number of wedges for runs that lasted several hours. Nonetheless, these images were still obtained for a Reynolds number below that of flight conditions at cruise.

Figure 2: Transition fixing philosophies used in the investigation

Configuration	Upper surface transition	Lower surface transition
Free	No trip	No trip
Lower surface tripped	No trip	Trip applied at 5% x/C
Upper and lower surface tripped	Trip at LE joint location	Trip at 5% x/C

Figure 3: Flow conditions used in ETW and CFD assessments

Mach	0.65	0.75	0.76
Reynolds (millions)	9, 12, 16	9, 12, 16	9, 12, 16

Figure 4: Illustration of transition fixing for different cases – upper surface

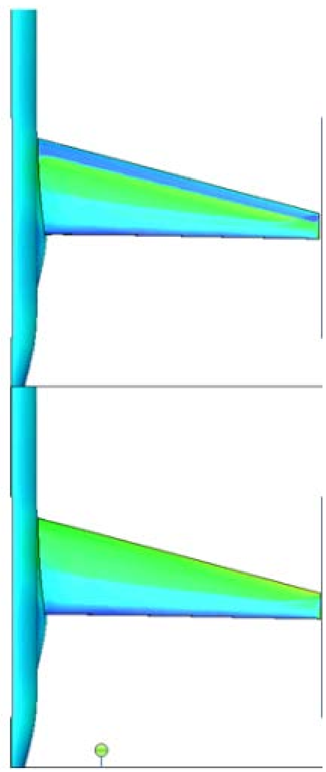

The upper image shows the transition fixed at the leading edge joint, in line with the approach used in the tunnel. The lower image shows the whole upper surface tripped.
Note that for the drag increments calculated between free and fixed transition, the reference case is that with transition at the

leading edge joint and thus still contains a short laminar extent on the upper surface.

Use of Temperature Sensitive Paint to determine transition position

Transition position during the test at ETW was assessed through the use of Temperature Sensitive Paint (TSP). The assessment technique was developed by the German Aerospace Center (DLR) [2-4] and the analysis of the images was performed by DLR engineers who participated in the ETW test entries.

Figure 5 shows an example of a TSP image taken at high Reynolds number in ETW. The dark areas in the images correspond to laminar flow, while the bright areas correspond to turbulent regions.

The location of laminar-turbulent transition is determined by finding the maximum intensity gradient of the grey value in the stream-wise direction.

The measured transition locations are marked with red dots.

Figure 5: Example of a Temperature Sensitive Paint image taken at ETW.

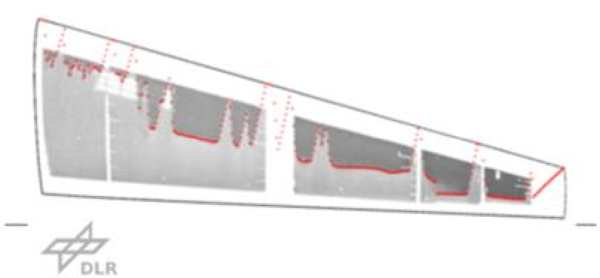

Computational approach:

Computations used the industrial standard RANS code Tau, from DLR.

Hybrid unstructured meshing was used with Airbus aerodynamic design standard meshing practice for laminar wings.

For simplicity of the mesh a free air simulation was used with no simulation of the tunnel walls or slots. It was not expected that representation of the tunnel geometry would enhance the calculation of the increment between free and fixed transition. In addition, although it was known that there could be half model effects on the pressures, particularly due to the large size of the model (semispan of the order of 1.5m), it was expected that the incremental trends between free and fixed transition would be captured for a free air simulation as they would not be particularly impacted by the half model effect.

Simulations were either performed with fixed transition or free transition as the solver could be coupled to a 2D linear e^N factor method for transition prediction.

Where simulations were performed with free transition, a flag was changed to set the upper wing surface as a free transition surface.

The initial transition position was set at a location in the far field. The transition prediction routine was called once for several hundred iterations.

When transition prediction was called, line-of-flight cuts were taken through the wing at pre-set locations. A boundary layer code computation was run on the pressures at each line-of-flight cut and the results assessed using an incompressible linear e^N method. The requirement of taking a complete line-of-flight cut through the wing to perform the boundary layer assessment led to the decision to locate the first cut outboard of the junction between the wing root and the belly fairing, consequently it was assumed that flow over the belly fairing was turbulent in the computations.

Upon completion of the e^N calculations, the updated transition position for each line-of-flight cut was passed back to the main code.

Results and Analysis:

Lift curve trends:

The tunnel measurements confirmed general trends seen in the CFD with respect to the benefit of laminarity on the upper surface for lift and pitching moment.

The principle effect seen was that at low lift co-efficient (CL), lift increased for a given angle of attack (alpha) when going from predominantly tripped to free transition on the upper surface, with additional gain in lift for a given alpha where supercritical flow developed on the bulk of the wing. This trend was seen both in the tunnel and CFD results at Reynolds number 16 million. At lower Reynolds number, similar behaviour was observed although the amount of lift gained from laminarity increased in comparison to the higher Reynolds numbers, e.g. at Reynolds number 9 million the increased level at low CL is 0.04 and at high CL is ~0.07. (Figures 6 -8)

The absolute level of the CL-alpha curves is not the same for the tunnel measurements and CFD results. This is probably due to the comparison being made between simulations without turbulent wedges taken into account and also limitations of the simulation e.g. half model effects, tunnel geometry, leakage that are not modelled. This is borne out by the fact that at Reynolds number of 9 million, where contamination is typically less, the agreement in results between ETW and CFD lift curves is better.

The lift gradients predicted by the CFD for tripped and untripped configurations agree well for all Reynolds numbers at low CL. At higher CL, the tripped turbulent solutions show a reduced gradient for the tunnel measurements in comparison to the CFD. However, the upper surface free transition curves show a change in gradient associated with supercritical flow development at the same CL for both CFD simulations and tunnel measurements, and the level of benefit is very similar. The trend is common for all Reynolds numbers simulated and measured.

Figure 6a: CL-alpha curve comparison of upper surface free and tripped results from ETW and CFD results, Reynolds number 16 million, M 0.75

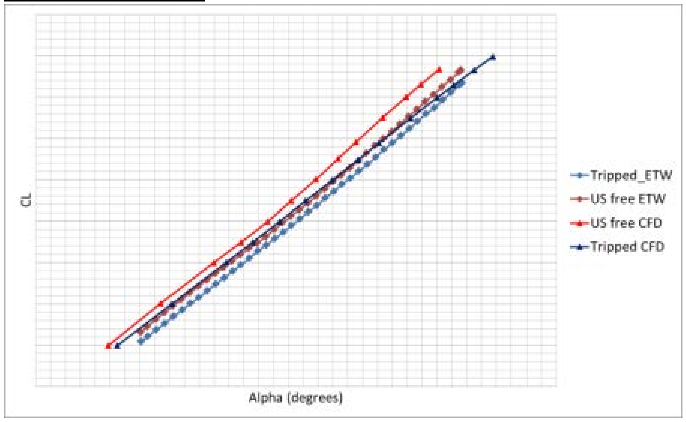

Figure 6b: DeltaCL-alpha upper surface free against tripped from ETW and CFD, Reynolds number 16 million M 0.75

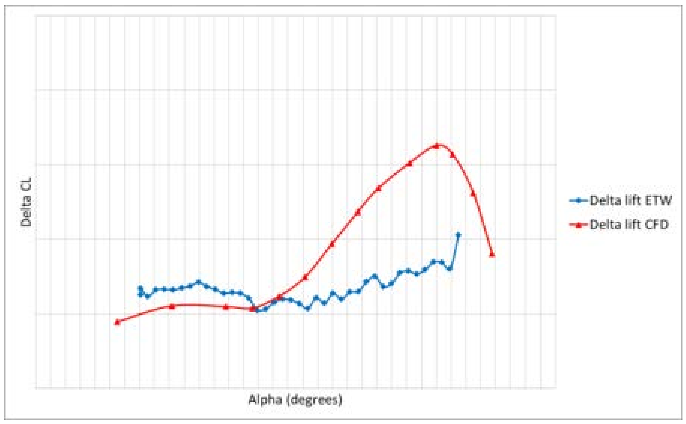

Figure 7a: CL-alpha curve comparison of upper surface free and tripped results from ETW and CFD, Reynolds number 12 million M 0.75

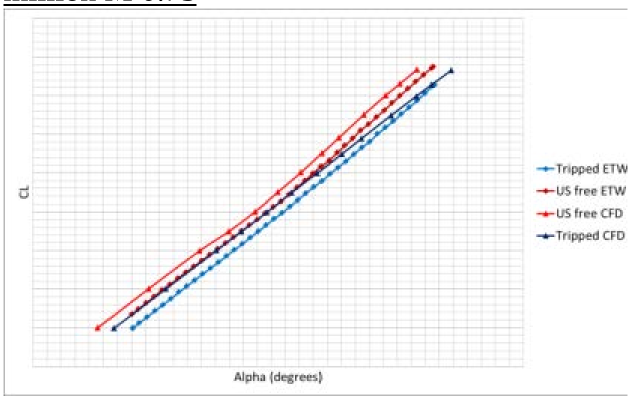

Figure 7b: DeltaCL-alpha upper surface free against tripped from ETW and CFD, Reynolds number 12 million M 0.75

Figure 8a: CL-alpha curve comparison of upper surface free and tripped results from ETW and CFD, Reynolds number 9 million M 0.75

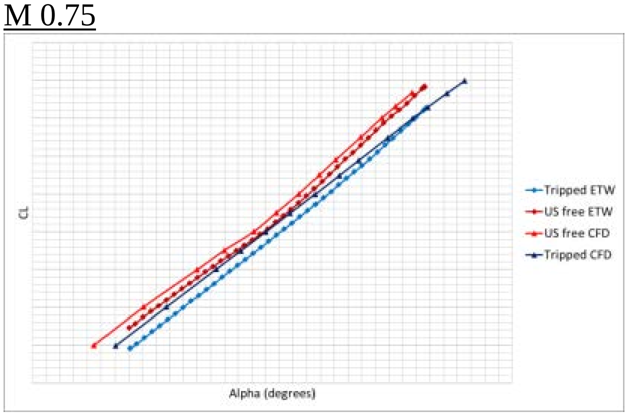

Figure 8b: DeltaCL-alpha upper surface free against tripped from ETW and CFD, Reynolds number 9 million M 0.75

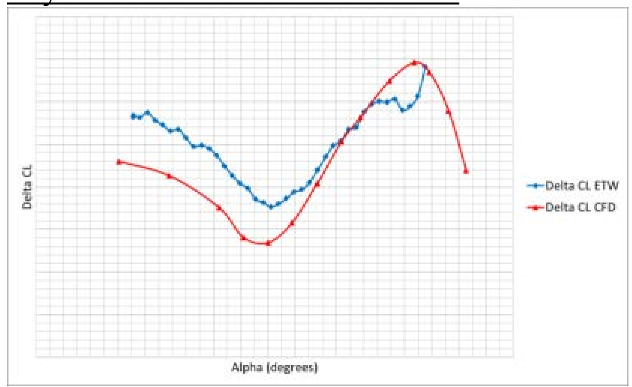

Pitching moment trends:

The pitching moment trends measured in the tunnel confirmed some features of the behaviour seen in CFD simulations, although the absolute level of the pitching moment was different.

The differences in absolute level between CFD and ETW measurements are smallest for the higher Reynolds number tripped upper and lower surface cases. (Figures 9 and 10) This would indicate that the level agrees well where the lift is dominated by the planform and spanwise loading.

For the cases where free transition occurs on the upper surface, the absolute level is different between ETW and CFD predictions. However, the tunnel measurements do confirm a phenomenon observed in the CFD predictions where the pitching moment gradient alters significantly where supercritical laminar flow develops. This would lead to a Natural Laminar Flow aircraft requiring a different trim philosophy for different CL as the pitching behaviour changes.

At Reynolds number 16 million, the CL at which the turning point of the pitching moment gradient occurs is similar but the

shape of the calculated curve is different from the curve measured at ETW, with lower pitching moment at high CL (Figure 9). However, at Reynolds number 12 million and 9 million, the shape of the curves measured in ETW and predicted by CFD matches quite well. (Figs 10 and 11)
Since the number of turbulent wedges on the wing is significantly less at Reynolds number 9 million this could indicate an effect linked to loading and pressure changes where the wing has locally turbulent regions.
It also verifies that the phenomenon seen in CFD is physical and can be predicted and with some further work to understand the source of the differences could be used to develop a useful trim model.

Figure 9a: Pitching moment-CL curve comparison of upper surface free and tripped ETW and CFD results, Reynolds number 16 million M 0.75

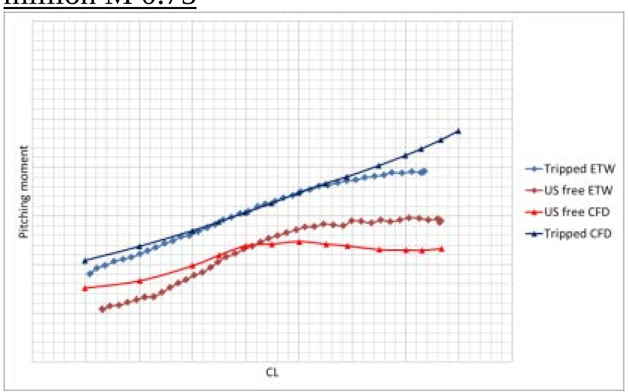

Figure 9b: Delta Pitching moment-CL curve comparison of effect of upper surface laminarity between ETW and CFD, Reynolds number 16 million M 0.75

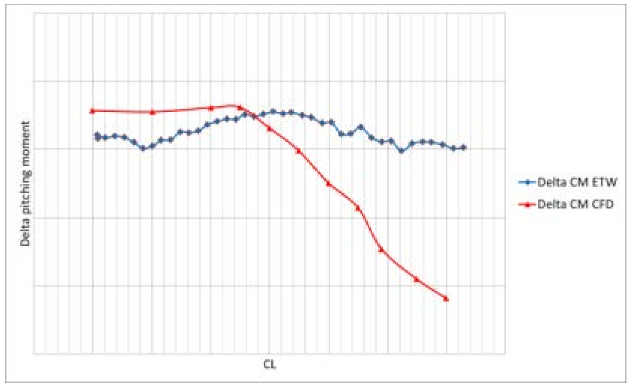

Figure 10a: Pitching moment-CL curve comparison of upper surface free and tripped results from ETW and CFD results, Reynolds number 12 million M 0.75

Figure 10b: Delta pitching moment-CL curve comparison of effect of upper surface laminarity ETW and CFD results, Reynolds number 12 million M 0.75

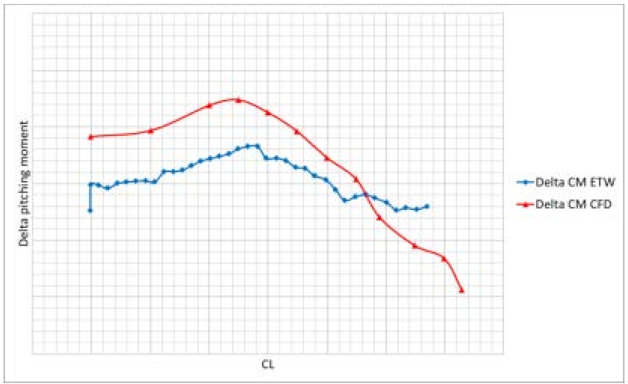

Figure 11a: Pitching moment-CL curve comparison of upper surface free and tripped results from ETW and CFD, Reynolds number 9 million M 0.75

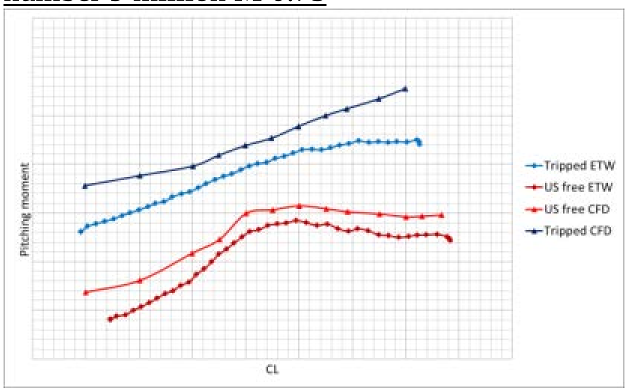

Figure 11b: Delta Pitching moment-CL curve comparison of effect of upper surface laminarity ETW and CFD results, Reynolds number 9 million M 0.75

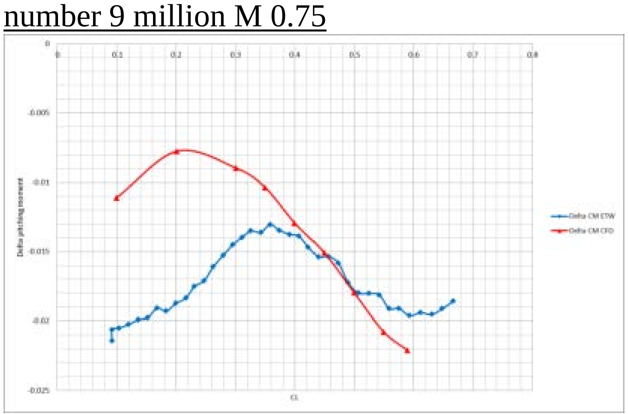

Assessment of drag delta due to upper surface laminar flow

It was known and expected that the absolute drag results for the large Natural Laminar Flow half model would not be comparable with those obtained for free air simulations. However, it was expected that incremental effects could be compared – in particular the drag benefit due to Natural Laminar Flow on the upper surface of the wing.
This was a useful increment to predict as it would give confidence in the level of aerodynamic benefit simulated for Natural Laminar Flow wing designs and enable a view of the worst case drag standard of the wing when the laminarity was compromised e.g. due to flying in clouds.

Figures 12 and 13 show that for both Reynolds numbers 16 and 9 million at M 0.76, the CFD predictions match the drag increment due to upper surface Natural Laminar Flow measured in ETW well at low CL. As the CL rises, the CFD simulations predict a rapidly increasing benefit of upper surface laminar flow upon drag which was not replicated in the tunnel.
Figure 14 shows that the bulk of this is from reduced viscous drag across the CL range as expected, with the benefit becoming larger at higher CLs as the effect of Natural Laminar Flow delays the drag rise. There is also a small delay to the wave drag rise.

From reviewing the TSP pictures taken during the test it was believed that the deviation could largely be explained by the presence of turbulent wedges removing proportionally more of the laminar extent as CL increases.
However, there was some concern that the relatively simple modelling of the effect of transition on boundary layer growth in CFD might lead to an optimistic view of the impact on drag. The CFD solver switches from one boundary layer growth rate to another upon reaching transition. This was known to be unphysical generally and

believed to be particularly unrepresentative of the boundary layer when transition occurred close to a shock.
Comparison of pressure distributions measured in the tunnel with pressure distributions from CFD with free transition showed that the CFD consistently predicts stronger shocks and higher acceleration after the shock than have been observed in ETW. Some differences in the pressures measured in the tunnel are inevitable due to the fact that the line-of-flight pressure tappings sit in a turbulent wedge. However, there was concern that the stronger shocks predicted by CFD might mean that as transition approached the shock, the CFD was predicting a larger benefit from laminar flow as there was proportionally higher drag to work on.

Figure 12: Delta due to laminar extent from ETW as a percentage of pre-test CFD prediction, M 0.76, Reynolds number 16 million

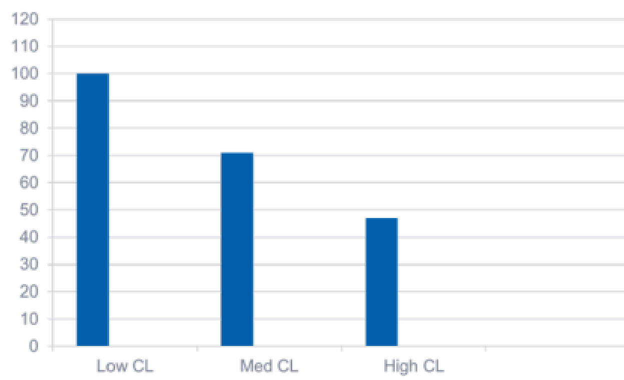

Figure 13: Delta due to laminar extent from ETW as a percentage of pre-test CFD prediction, Reynolds number 9 million, M 0.76

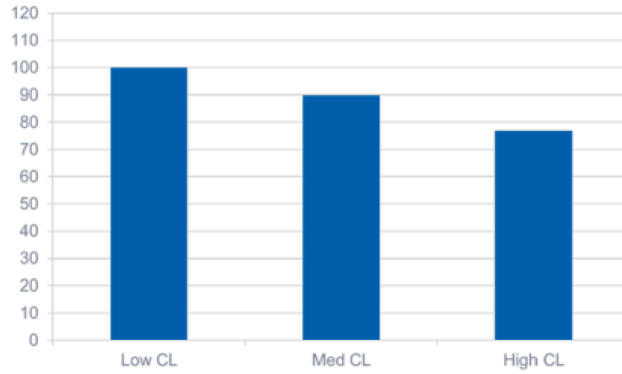

Figure 14: Viscous drag-CL compared for upper surface free transition and both surfaces fixed transition from CFD, Reynolds number 9 million, M 0.76

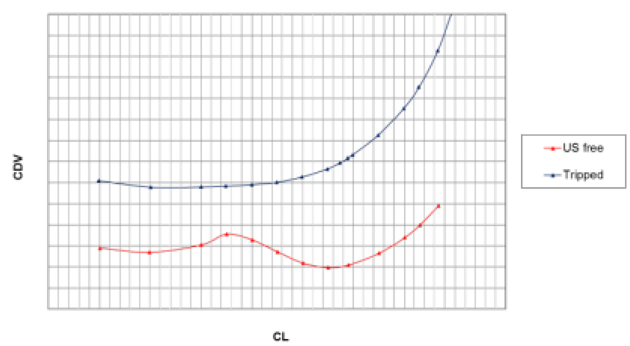

CFD investigation of the effect upon drag increment of transition approaching the shock

To eliminate the effect of factors other than turbulent wedges affecting the comparison of CFD and tunnel Natural Laminar Flow increments, a study was undertaken in CFD. Simulations were performed with transition fixed at a constant chordwise position across the span for several positions up to the shock. The resulting drag increment due to upper surface laminar flow was plotted for all the cases alongside the increment derived from free transition.
It was hypothesised that the simplistic modelling of the boundary layer changes at transition would mean that close to the shock a sudden change in drag increment

would occur. However, as Figure 15 shows, the increasing Natural Laminar Flow increment rose in proportion to increasing chordwise position. The free transition simulation which at high CL indicated shock limited transition did not diverge significantly from the fixed transition results.

Figure 15: Percentage of free transition increment due to upper surface Natural Laminar Flow for different chordwise transition extents from CFD, M 0.76, Reynolds number 16 million

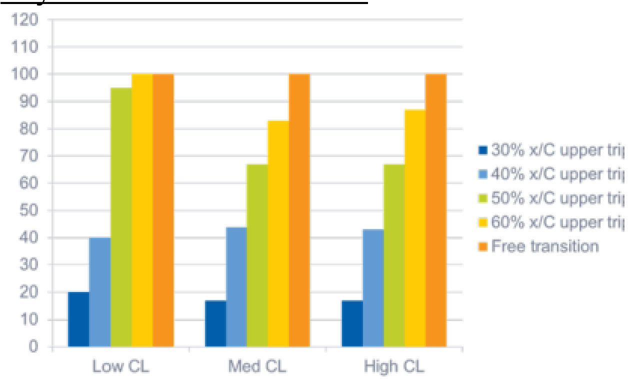

The conclusions of this analysis are that despite the simple modelling of the change in boundary layer growth rate employed in CFD, there appears to be sufficient capture of the flow physics to give a real indication of expected laminar benefit where transition occurs close to a shock.

CFD investigation of modelling the impact of flow contamination measured in the tunnel on the Natural Laminar Flow drag increment.

Having eliminated weaknesses in the CFD simulations as the reason for differences in the Natural Laminar Flow delta obtained from CFD against the delta measured in the tunnel, attention returned to the effect of turbulent wedges on the drag increment.
To get as representative a comparison as possible between the CFD and the wind tunnel results, the TSP images recorded for different CLs in the tunnel were used to obtain the measured transition position.
CFD simulations were then performed for individual CLs with the measured transition position set.
The drag delta between these simulations and simulations of the upper surface tripped at the leading edge joint, lower surface tripped at 5% x/C was calculated.
These deltas were then compared with the delta measured in the tunnel.
Figures 16-18 show the TSP images with the measured transition position compared to the CFD simulation of the same transition position.
There are limitations to the modelling of the measured transition position. The transition prediction assessment relies upon taking line of flight cuts through the wing. Close to the wing root, this leads to issues where the belly fairing intersects the wing and has not been set as a transition surface, so the first spanwise station has to be set slightly outboard of the wing root/belly intersection.
Also, the front of the turbulent wedge cannot be fully represented as individual cells in the mesh cannot be both turbulent and laminar, thus the turbulent wedges tend to have blunter leader edges than the measured transition from the tunnel.
However, despite these limitations, the representation of the measured transition captures the flow contamination well.

Figure 16: Low CL, M0.76, Reynolds number 16 million, skin friction contours from CFD compared to TSP image from CFD

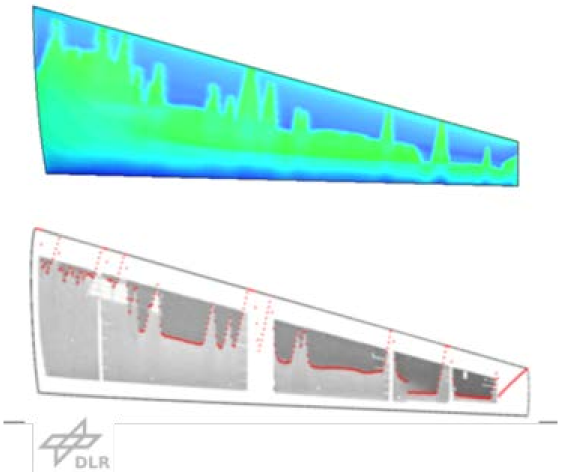

Figure 17: Intermediate CL, M0.76, Reynolds number 16 million, skin friction contours from CFD compared to TSP image from CFD

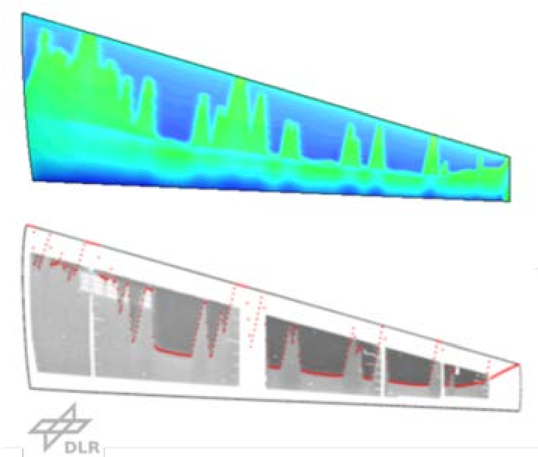

Figure 18: High CL, M0.76, Reynolds number 16 million, skin friction contours from CFD compared to TSP image from CFD

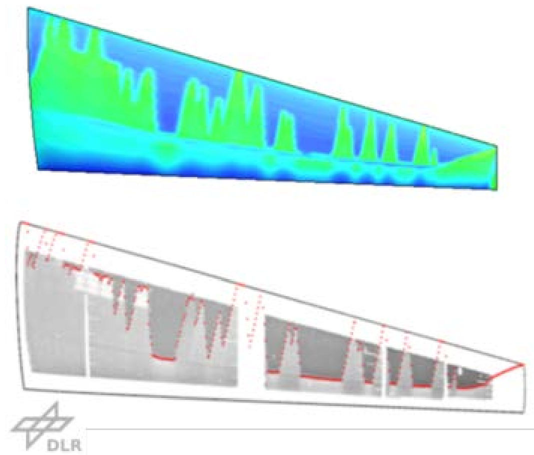

When the drag delta due to upper surface laminar extent obtained from these simulations is compared with the ETW results, the agreement is reasonably good and consistent across the CL range, with a constant offset of ~4 drag counts (dc). (Figure 19)

Since this level of agreement is consistent up to higher CLs, it indicates that the driving factor in lack of agreement between a clean free transition based delta and the ETW delta is the effect of turbulent wedges. Since the transition fixing was sized for Reynolds number 12 million, there was some evidence from the TSP images of overfixing at Reynolds number 16 million. This would lead to a drag penalty which would explain part of the constant offset. This is also borne out by the fact that when the exercise was repeated for Reynolds number 9 million, the match between the CFD simulations with measured transition and the tunnel data was closer. (Figure 20) Remaining differences are probably due to the limitations of the modelling described earlier.

Figure 19: ETW drag increment due to laminarity as a fraction of CFD with measured transition simulated M 0.76, Reynolds number 16 million

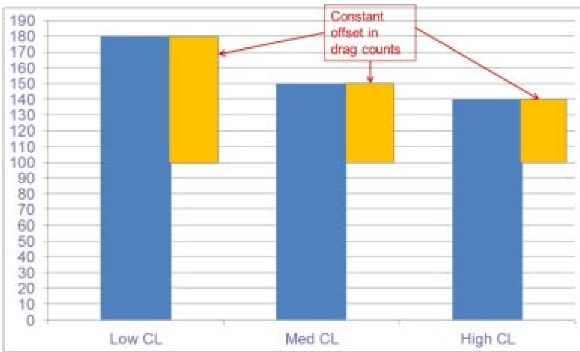

Figure 20: ETW drag increment due to laminarity as a fraction of CFD with measured transition simulated M 0.76, Reynolds number 9 million

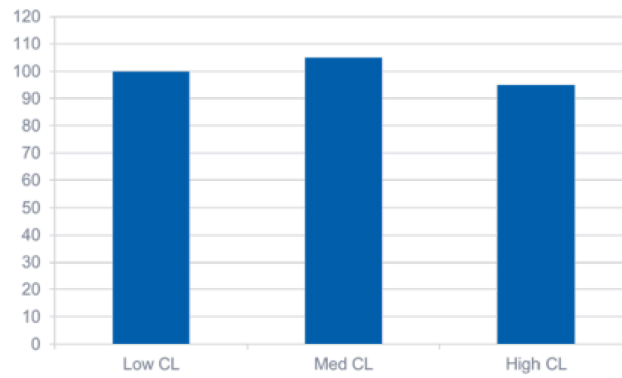

Simulation of additional CLs at a Reynolds number of 9 million showed an outlier in the comparison of deltas at low CL for M 0.76. The ETW drag increment was 156% of the CFD simulation with measured transition modelled. Thus the simulation was predicting a smaller benefit due to Natural Laminar Flow than the wind tunnel data. Figure 21 compares the skin friction (CFX) plot with the measured transition for this case with the TSP image. The comparison shows that not all of the features in the TSP image have been captured in the CFD representation. This demonstrates that failure to capture the transition for small areas can nonetheless have a measurable impact on the calculated drag impact.

Figure 21: Intermediate CL, M 0.76, Reynolds number 9 million, CFX contours from CFD compared to TSP image

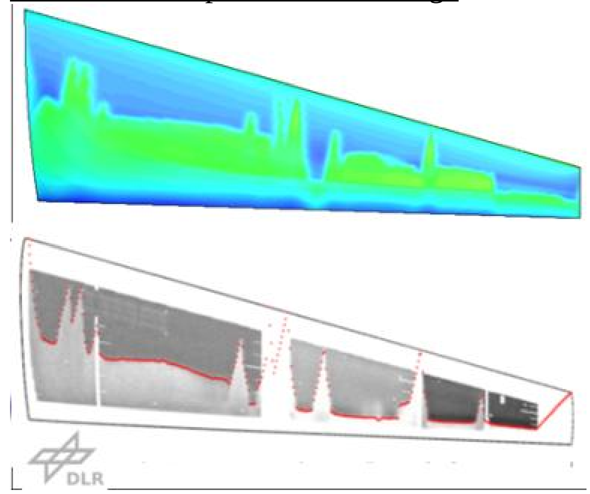

Conclusions:

Simulations have been performed in RANS CFD to represent the tripping philosophies of a X0010RP1623750 Natural Laminar Flow half model in ETW using a free air model.

Simulations were performed both for a clean, uncontaminated wing and with transition set to represent the measured transition from ETW.

Comparison of lift curves obtained from the tunnel and from CFD confirm the physicality of changes in the lift gradient at the onset of supercritical flow for free transition conditions.

Comparison of pitching moment curves obtained from the tunnel and from CFD simulations show good agreement for the tripped, turbulent wing at Reynolds number 16 million and 12 million for a large range of CL.

The same comparison performed for free transition on the upper surface confirm the physicality of a gradient change at the onset of supercritical flow where both CFD and wind tunnel predict consistent gradient trends for Reynolds number 9 million and consistent turning points for higher Reynolds number.

The simulations with transition set based upon ETW measurements show good agreement with the measured drag increments at most CL for Mach 0.76 at Reynolds number 9 million
At Reynolds number 16 million, the CFD simulations with measured transition are 4-5 counts more conservative than the measured ETW increment but show a similar trend. This shows better agreement than the clean wing free transition simulation. The offset is probably due to a drag penalty due to overfixing in the ETW data.
This verifies that the drag increment due to Natural Laminar Flow measured in wind tunnel tests at high Reynolds number and cruise Mach number can be predicted to a reasonable level of accuracy by CFD provided flow contamination is represented.

CFD investigation of the difference in drag delta for increasing chordwise Natural Laminar Flow extent against free transition verified that there is no significant deviation in drag features where transition approaches the shock, despite the simple modelling of the boundary layer growth rate.

Together, these conclusions indicate that free air simulations of a Natural Laminar Flow wing using an industrial RANS code coupled to a linear e^N transition prediction method can provide a representative view of the drag benefit due to laminar flow and the impact on that benefit of flow contamination.

References:

1) ACARE 2020: Meeting society's needs and winning global leadership - Report of the Group of Personalities, Jan 2001, Arguelles P., Lumsden J., et al
2) U. Fey, R. H. Engler, Y. Egami, Y. Iijima, K. Asai, U. Jansen, and J. Quest: "Transition Detection by Temperature Sensitive Paint at Cryogenic Temperature in the European Transonic Wind Tunnel (ETW)", 20th ICIASF, Record, 2003, pp.77-88.
3) Y. Iijima, Y. Egami, A. Nishizawa, K. Asai, U. Fey, and R. H. Engler, "Optimization of Temperature-Sensitive Paint Formulation for Large-Scale Cryogenic Wind Tunnels", 20th International Congress on Instrumentation in Aerospace Simulation Facilities(ICIASF), Record, 2003, pp.70-76.
4) U. Fey and Y. Egami in: Tropea, Yarin, Foss [Eds.] "Springer Handbook of Experimental Fluid Dynamics", Springer Verlag, 2007 (Chap. 7.4: "Transition Detection by Temperature-Sensitive Paint")

Acknowledgements:
TSP images are reproduced by kind permission of DLR.